

Iris as a reflector for differential absorption low-coherence interferometry to measure glucose level in the anterior chamber

Yong Zhou,^a Nan Zeng,^a Yanhong Ji,^b Yao Li,^a Xiangsong Dai,^a Peng Li,^a Lian Duan,^a Hui Ma,^a and Yonghong He^a

^aTsinghua University, Laboratory of Optical Imaging and Sensing, Graduate School at Shenzhen, Shenzhen, 518055, China

^bSouth China Normal University, MOE Key Laboratory of Laser Life Science & Institute of Laser Life Science, Guangzhou 510631, China

Abstract. We present a method of glucose concentration detection in the anterior chamber with a differential absorption optical low-coherent interferometry (LCI) technique. Back-reflected light from the iris, passing through the anterior chamber twice, was selectively obtained with the LCI technique. Two light sources, one centered within (1625 nm) and the other centered outside (1310 nm) of a glucose absorption band were used for differential absorption measurement. In the eye model and pig eye experiments, we obtained a resolution glucose level of 26.8 mg/dL and 69.6 mg/dL, respectively. This method has a potential application for noninvasive detection of glucose concentration in aqueous humor, which is related to the glucose concentration in blood. © 2011 Society of Photo-Optical Instrumentation Engineers (SPIE). [DOI: 10.1117/1.3528658]

Keywords: differential absorption; low-coherent interferometry; iris; glucose; noninvasive.

Paper 10295RR received May 31, 2010; revised manuscript received Nov. 22, 2010; accepted for publication Nov. 30, 2010; published online Jan. 20, 2011.

1 Introduction

Noninvasive sensing methods for determining glucose concentration in biological fluids have been under investigation for more than 30 years.¹ These approaches include the glucose absorption measurement with near infrared (NIR) spectroscopy,² photoacoustic spectroscopy,^{3,4} and tissue scattering measurement with optical coherence tomography (OCT).⁵ As most measurement sites are blood-containing tissue on external body (e.g., skin, finger, earlobe, lip),⁵⁻⁷ these techniques face problems such as the complexity of human tissue, pulsatile nature of blood flow, unstable temperature^{8,9} and effect of skin pressure¹⁰ etc. Up to now, few repeatable and quantifiable results have been reported *in vivo*. It is well known that there is a good correlation between glucose levels in aqueous humor and in blood.¹¹ Because aqueous humor in the anterior chamber of the eye is, optically, a more accessible glucose-containing body fluid, it is suggested that aqueous humor could be served as a surrogate for blood for noninvasive analysis of glucose concentration.

Several research groups have proposed and studied approaches to monitor glucose concentration in the aqueous humor. These techniques include polarization changes, Raman spectroscopy, and iris imaging analysis. In 1999, Cameron et al.¹² used polarization rotation of light through the eye to measure glucose concentration. Recently, Malik et al.^{13,14} achieved a resolution of 12.8 mg/dL in the cuvette experiments with real-time closed-loop dual-wavelength optical polarimetry. In 2005, Lambert et al.¹⁵ and Pelletier et al.¹⁶ utilized Raman spectroscopy in combination with partial least squares (PLS) analysis to quantify glucose concentration and achieved a root-

mean-square error of 22 mg/dL in artificial aqueous humor experiment. In 2010, Webb et al.¹⁷ reported a multivariate image processing technique for noninvasive glucose sensing. Based on the refractive index change of aqueous humor induced by glucose concentration,¹⁸ they created a calibration model to predict glucose concentration by analyzing iris images.

Since it was introduced in 1991,¹⁹ OCT has been proven to be an important modality for micrometer-scale imaging. In recent years, many groups have worked on expanding OCT to functional imaging. Promising results have been reported in Doppler flow imaging, polarization sensitive OCT, and spectroscopic OCT. Several authors have addressed the challenge of extracting quantitative information on optical properties using low coherence interferometry (LCI) and OCT. Michael Pircher et al. reported differential absorption OCT to measure water concentration in human cornea.²⁰ It was also reported the measurement of dye diffusion in scattering tissue phantoms using dual-wavelength LCI.²¹

The motivation of this work is to monitor glucose concentration in the anterior chamber of eye with a differential absorption low-coherent interferometry (DALCI) technique. We selectively obtain the signals scattered from the iris by LCI technique. The light scattered from the other parts can therefore be eliminated, especially the strong light reflected from the cornea. As a result, the LCI technique has a relatively high signal-to-noise ratio, as well as a relatively high resolution in quantification measurement. In addition, since aqueous humor can be treated as non-scattering medium in the wavelengths that we used in this work, the influence due to scattering can be ignored.²² According to the absorption band of glucose and water,²³ we developed a DALCI using two different light sources, one centered within

Address all correspondence to: Yannong Ji and Yonghong He, Tsinghua Univ., D307A Xili Univ. Town, Shenzhen, Guangdong 518055, China. E-mail: jiyh@scnu.edu.cn; heyh@sz.tsinghua.edu.cn

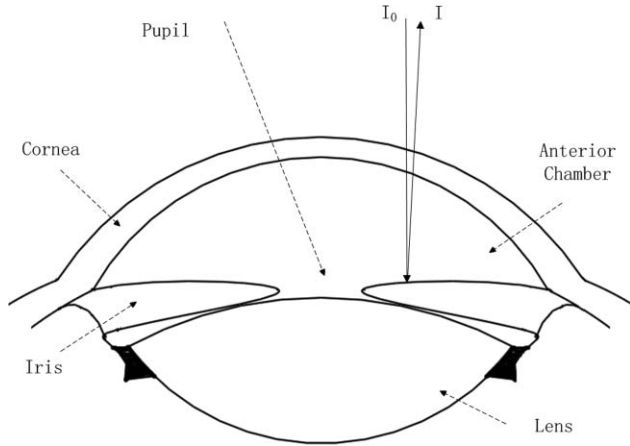


Fig. 1 The structure of anterior chamber. An incident light I_0 gets into the anterior chamber. After passing through the aqueous humor, the emergent light I is scattered back from the iris. Being absorbed twice by glucose in the aqueous humor, the emergent light I carries the information of glucose concentration.

(1625 nm) and one centered outside (1310 nm) of a glucose absorption band, to measure glucose level in the anterior chamber of a pig eye *ex vivo*.

2 Principle

The anterior chamber is located between the cornea and the lens, with the thickness of 3.13 ± 0.50 mm.²⁴ It is filled with transparent liquid—aqueous humor, with a total volume about $250 \mu\text{L}$.²⁵

Figure 1 shows the structure of a typical anterior chamber. A light beam with intensity I_0 passes through the aqueous humor in the anterior chamber of the eye. Since the cornea and aqueous humor are nearly optically transparent, the iris could be treated as a natural reflector to scatter the beam back. The intensity I of the scattered beam from the iris after propagating through twice of thickness z of the aqueous humor can be described by Beer's law

$$I(\lambda, 2z) = I_0(\lambda)e^{-2[\mu_a(\lambda)+\mu_s(\lambda)]z}, \quad (2.1)$$

where λ denotes the wavelength, μ_a the absorption coefficient and μ_s the scattering coefficient. By utilizing LCI, the weak backscattering optical signal from a particular layer of medium can be obtained with high sensitivity. Here, we adopted a dual-wavelength LCI to selectively detect the light scattered back from the iris. Two different light sources were selected one centered within (1625 nm, λ_1) and the other centered outside (1310 nm, λ_2) of an absorption band of glucose.

The theory of differential absorption LCI was established in Ref. 20. The relation between signals of two wavelengths LCI and the differential absorption coefficient $\Delta\mu_a$ and scattering coefficient $\Delta\mu_s$ can be expressed as

$$\ln R = \text{Const.} - (\Delta\mu_a + \Delta\mu_s)z, \quad (2.2)$$

where R is the ratio of two wavelengths LCI signals denoted as

$$R = \frac{S_{LCI}(z, \lambda_1)}{S_{LCI}(z, \lambda_2)}, \quad (2.3)$$

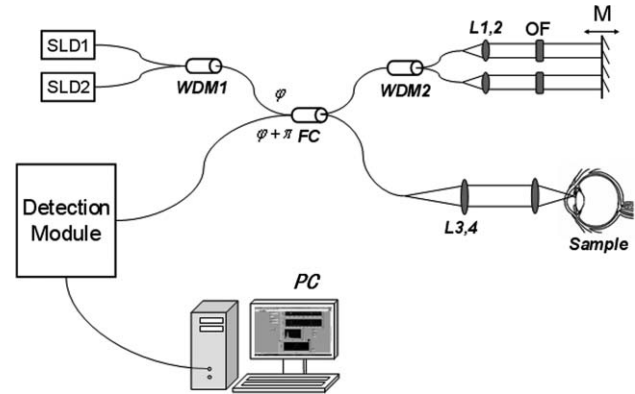


Fig. 2 Schematic diagram of the differential absorption LCI system with two wavelengths (SLD1, $\lambda_1 = 1310$ nm; SLD2, $\lambda_2 = 1625$ nm; FC, 2X2 fiber coupler; OF, optical filter; WDM1, wavelength division multiplexer; WDM2, wavelength demultiplexer; M, vibratile mirror; L, lens).

where $S_{LCI}(z, \lambda_1)$ is the LCI signal of 1625 nm light, $S_{LCI}(z, \lambda_2)$ is the LCI signal of 1310 nm light, and z is the thickness of the aqueous humor.

In our experiments, the cornea and aqueous humor can be treated as nearly non-scattering substance. The difference in the absorption coefficient is much larger than the difference in the scattering coefficient, thus the influence of scattering can be neglected. The differential absorption cross section $\Delta\sigma_a$ can be measured by the conventional spectroscopy. Equation (2.2) can be reduced to

$$\ln R = \text{Const.} - (\Delta\sigma_a z)C. \quad (2.4)$$

Equation (2.4) is a linear function in C and the slope are decided by $\Delta\sigma_a$ and z . The concentration C can be predicted by the two wavelength LCI signals.

3 Materials and Methods

The DALCI setup, shown in Fig. 2, is a fiber based Michelson interferometer. Two different low coherence light sources were coupled by a wavelength division multiplexer (WDM) at the interferometer entrance. For this work we used two fiber pigtailed SLDs (Denselight Inc., Singapore) with center wavelengths at 1310 nm (FWHM bandwidth $\Delta\lambda = 50$ nm) and at 1625 nm (FWHM bandwidth $\Delta\lambda = 50$ nm), respectively. The emission powers and coherence length were 5 mW, $15.1 \mu\text{m}$ for the 1310 nm light source and 10 mW, $23.3 \mu\text{m}$ for the 1625 nm light source in the air, respectively. These two wavelengths were separated by a WDM into two reference beams. To eliminate the two wavelengths cross interaction in the WDM, two optical bandpass filters and two optical switches were placed in the corresponding reference beam. The reference mirror was driven by a servo motor, which was well controlled and synchronized by a personal computer. When the motor moved forward and backward, the beam of 1310 and 1625 nm switched on separately, allowing the same detector to record the coherence signals of the interferometer of such two wavelengths separately. The spectra responses of the detector to light with center wavelengths at 1310 and 1625 nm were 0.94 and 1.01 A/W, respectively. Normalization was conducted during calculation of the ratio R . An objective lens (10/0.25, 160/0.17) was used

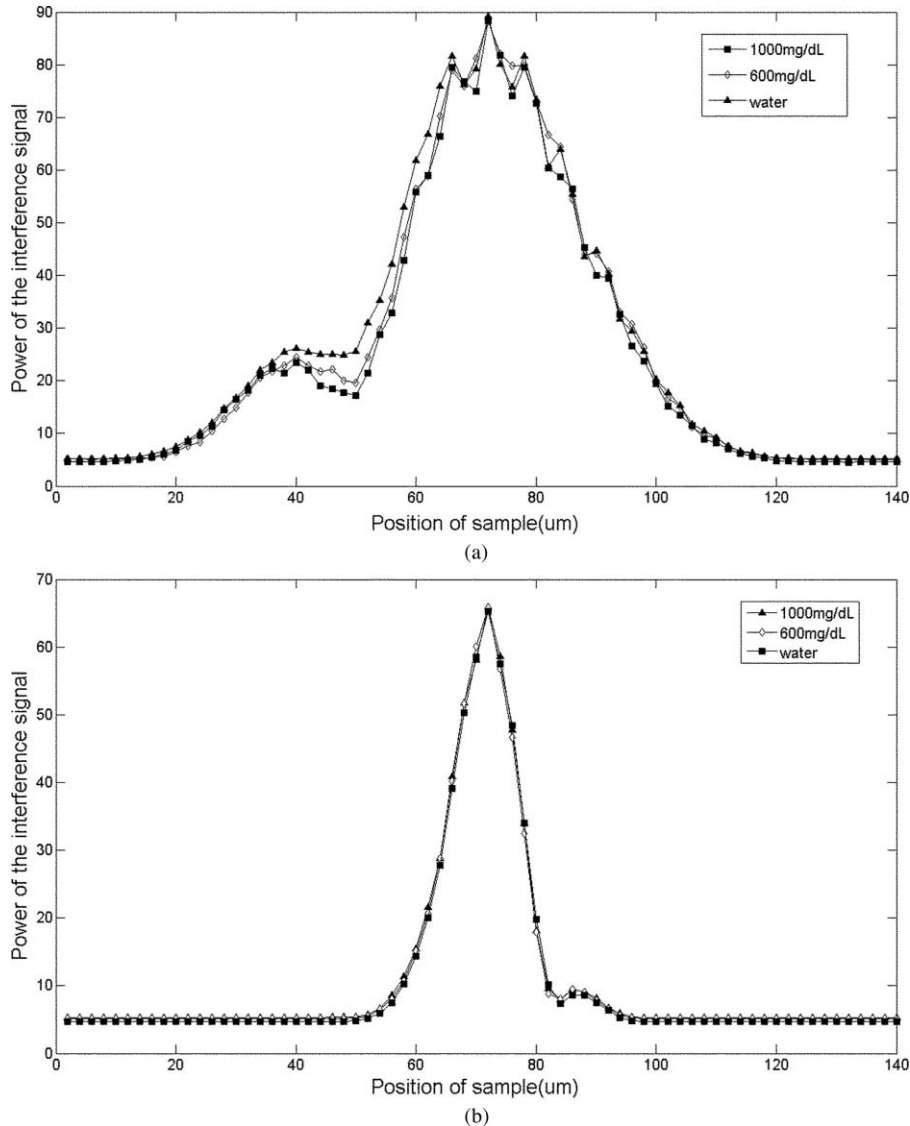


Fig. 3 The sample was a pig eye which had been *ex vivo* less than 4 hours. (a) The different intensity of interference signals of the wavelength 1625 nm; (b) The basically unchanged intensity of interference signals of the wavelength 1310 nm.

in sample arm to focus light on the sample. The electronic filter of the detector was set to be 2 kHz to improve signal-to-noise ratio. This required that the motor moved forth and back with different velocity. When we recorded interferometric signals with center wavelengths at 1310 and 1625 nm, the scanning speeds of the reference mirror were set to 0.91 and 0.74 mm/s, respectively.

In the experiments, we prepared a set of glucose water solution with concentrations of 0, 100, 200, 300, 400, 500, and 600 (mg/dL). To reduce the speckle noise, we took an average value by recording 30 coherence signal ratios (R) from the DALCI for each sample measurement. Every sample was measured four times to take the effect of the external environment into account. A weighted average of these four measurements was used as the final results.²⁶ In the pig eye experiments, we used the fresh native pig eyes which had been *ex vivo* for less than 4 hours. The fluid in the anterior chamber with glucose solution was replaced by home-made infusion device including an eye clamp to maintain the structure of the anterior chamber and

the depth z unchanged throughout the experiments to minimize motion influence.

4 Results and Discussions

The LCI signals of the iris were shown in Fig. 3 to prove the feasibility of our experiment. The sample was a pig eye which had been *ex vivo* less than 4 hours. We recorded 30 signals in each measurement and averaged these signals over four measurements. In Fig. 3, the vertical and lateral axis represent the intensity of LCI signals (A-scans) and position of the scanning mirror in the reference arm, respectively, which corresponds to the real position of sample. As is shown in Fig. 3(a), due to the absorption by glucose, the intensity of LCI signal in 1625 nm is becoming smaller with the increase of glucose concentration. The signal attenuation is obvious where x -coordinate is 50 μm . We integrated the signals from 40 μm to 110 μm of x -coordinate in the experiment. By contrast, as is shown in Fig. 3(b), the

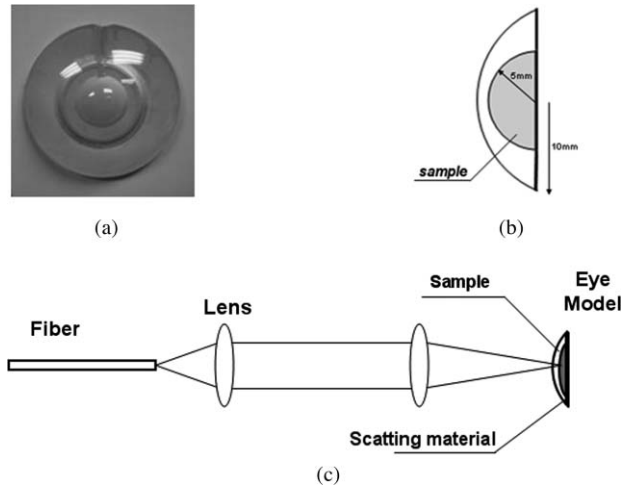


Fig. 4 The eye model experiment. (a) The photo of eye model. (b) The structure of eye model. (c) The diagram of the optical path in the sample arm.

signal intensity of 1310 nm is basically unchanged when glucose concentration is increased. The difference of refractive index resulting from the two wavelengths is about 1.408×10^{-3} , while the relationship between the change of refractive index and glucose concentration is $\Delta n = 1.52 \times 10^{-6}$ per 1 mg/dL glucose.²⁷ Thus, the optical path length induced by the difference of refractive index is negligible, which is also shown in Fig. 3 that the signals' position remains almost the same whatever the wavelengths and the glucose concentrations are.

With the goal to measure glucose concentration in aqueous humor, we made an eye model to simulate the structure of anterior chamber. As shown in Figs. 4(a) and 4(b), the model was composed of a glass hemispherical shell and the scattering background which was a piece of white paper pasted on the shell. The glass hemispherical shell we used was similar to the anterior chamber in structure. Figure 4(c) shows the sample arm in these experiments. The light was focused on the center of the model. The thickness z in this experiment was 5 mm.

The resolution δC can be expressed as

$$\delta C = \frac{\Delta C}{\Delta R} \delta R, \quad (4.1)$$

where ΔC is the concentration difference (100 mg/dL in the experiment), ΔR is the average difference of R , and δR is the mean value of the standard deviation in each measurement.

After we measured a series of glucose water solution, seven groups of data were recorded. Taking a weighted average over each group, R was plotted in Fig. 5(a). As shown in Fig. 5(a), the resolution calculated by Eq. (4.1) in the shell experiment was 26.8 mg/dL and the root-mean-squared error of prediction (RMSEP) was 28.45 mg/dL. We also plotted $-\ln R$ in Fig. 5(b). After linear fitting of the data points, the correlation coefficient was 0.9944.

We used a fresh pig eye as the test sample which had been *ex vivo* less than 4 hours [Fig. 6(a)]. The biodiversity was not taken into account in the result. Fig. 6(b) shows the sample arm in this experiment and the light was focused on the edge of iris. A commercial OCT system (OSE-1400, Moptim Inc., China) was used to measure the thickness z of the pig eye in our experiment. The OCT image of pig eye is shown in Fig. 6(c).

The axial spatial resolution of the commercial OCT system was about $8 \mu\text{m}$. The thickness z was about 1.65 mm. The error in concentration resulting from the error in z was about 0.5% of the absolute concentration value. We exchanged the fluid in the anterior chamber with an infusion device [Fig. 6(d)]. Each of the glucose water solution was measured once in 2 min.

After we measured a series of glucose water solution, we still recorded seven groups of data. The average R of each group was plotted in Fig. 7(a). As shown in Fig. 7(a), the resolution we calculated in this experiment was 69.6 mg/dL and the RMSEP was 65.62 mg/dL. We also plotted $-\ln R$ in Fig. 7(b), after linear fitting of the data points, the correlation coefficient was 0.9931.

The influence induced by other materials, such as water, proteins, ascorbic acid, and melanin in the aqueous humor, were not taken into account. Among such interferents, the impact of water is the most significant, as it has a higher absorption than other materials. Moreover, it is the main constitute of aqueous humor, which is as high as 99%.²⁸ To minimize the influence of water, we used two light sources with center wavelengths at 1310 and 1625 nm where the absorption of water is relatively equal and low, while the absorption difference of glucose is relatively high.^{29,30} It has been proved that the glucose concentration in the aqueous humor is two orders of magnitude higher than other optically active substances.³¹ Meanwhile, the absorption coefficient of glucose at these wavelengths is larger than other substances.^{30,32-35} In order to reduce the remaining little influence of water and other materials, two possible methods can be considered to solve this problem. One is multivariate calibration techniques³⁶⁻³⁸; the other is to use a closed-loop system.³⁹ Both of them have been demonstrated to be able to compensate for the interference due to other materials potentially.

The absorption coefficients of water and glucose solution do not remain the same under different temperatures. In our experiment, each sample was used in the experiment until they reached the same temperature. Located deep in the eyes, the change of temperature of iris is much smaller than that of the external bodies, such as skin, earlobe, etc., which are often used in current detection. Another vital influence of the measurement is the flowing status of liquid. According to the observation and calculation in the experiment, we observed significant difference in the absorption coefficient if the flowing status of solution was different. Generally, the solution would become static in 2 min after every replacement of new solution. In our future experiments *in vivo*, since the producing rate of aqueous humor is about $3.1 \mu\text{l}/\text{min}$ in the daytime,⁴⁰ it keeps a dynamic equilibrium and the flowing status basically stays unchanged. As a result, the errors introduced by the liquid flowing can be ignored.

Because of the different scattering properties of different scattering locations, the focusing position of incident light should keep unmoved especially in the pig eye experiment to maintain the deepness z unchanged. To reduce the errors induced by the movement of imaging spot, all experiment equipments were fastened tightly on the optical table and a non-touching replacing solution trick is very important in the *ex vivo* experiment. To reduce the impact of the movement of focusing position further, the incident light should not focus exactly on the iris. If we exclude the limitation of intensity detection, the best choice is to use parallel mode in the *in vivo* experiments. Another efficient solution to reduce the influence of the movement of imaging spot is to utilize rapid scanning optical delay (RSOD) instead of

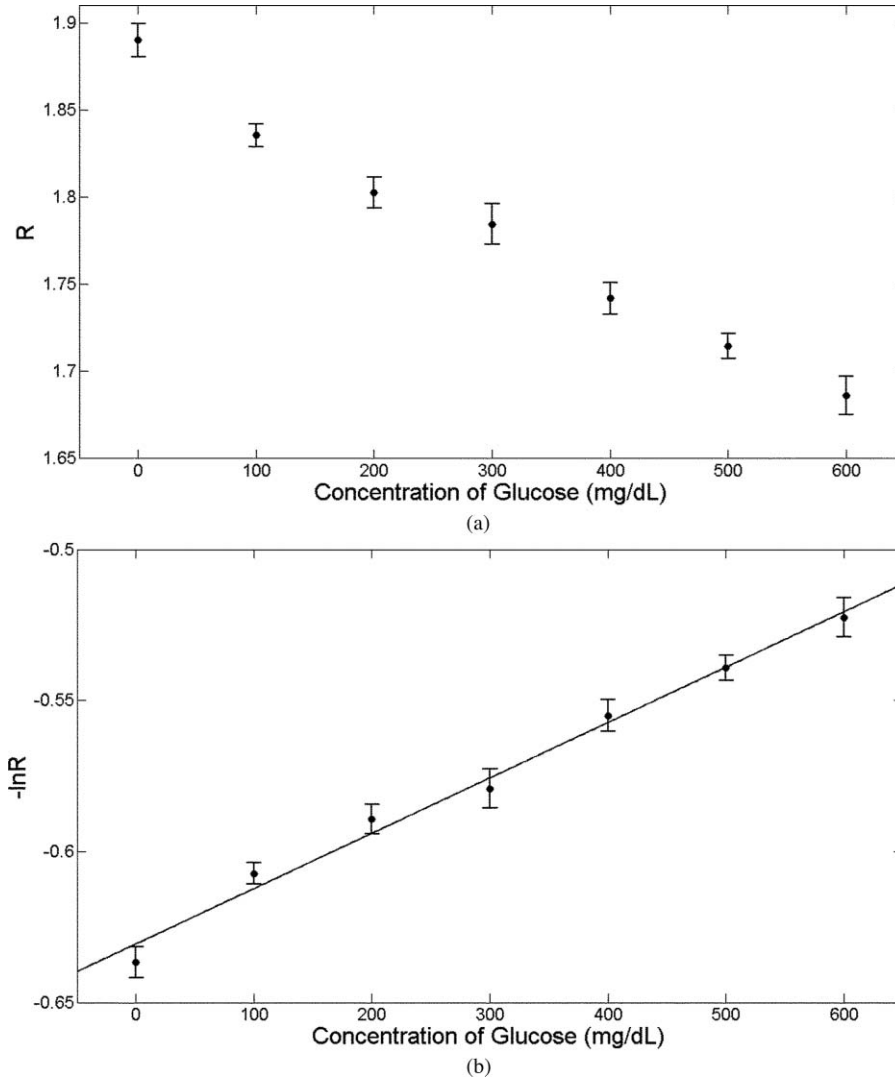


Fig. 5 The measurement results for the eye model experiment. (a) The R is shown versus glucose concentration. An average of thirty R within two minutes was recorded as a sample measurement. In order to reduce the impact of the external environment, the weighted average of four times measurement was calculated as the final results. The resolution was 26.8 mg/dL, and the RMSEP was 28.45 mg/dL. (b) The $-\ln R$ is shown versus glucose concentration. The linear correlation between C and $-\ln R$ was 0.9944.

a mirror driven by motor as the reference arm. Currently, a total 120 s are needed to acquire 30 signals. We can reduce measurement time by using RSOD to obtain hundreds of signals within a second.

We use calibration curves to measure glucose concentration currently. According to Eq. (2.2), the slope of the curve is determined by z . Since z is different in the shell and pig eye experiment, the slopes in Figs. 5(b) and 7(b) are different. From the calibration curves, we can obtain the relationship between $-\ln R$ and glucose concentration C . The value of z does not exert influence on the final results while it produces impact on the theoretical resolution in our experiments. We can calculate such curves with the absolute values of $\Delta\mu_a$ and z instead of obtaining a calibration one for each patient. The only step required is to measure every patient's anterior chamber structure by OCT to obtain the absolute value of z .

According to the Eq. (2.2), the resolution is determined by $\Delta\mu_a$ and z and may increase if we have a higher value of $\Delta\mu_a$ or z . Based on the experiments we have done, two ways

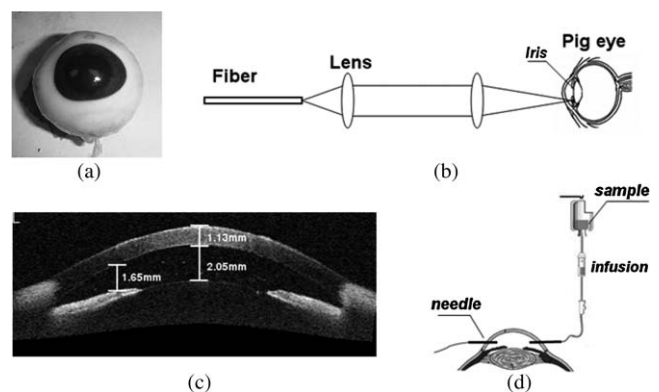


Fig. 6 The pig eye experiments: (a) The photo of sample we used in this experiment. (b) The diagram of the optical path in the sample arm. (c) The OCT image of the pig eye we use. The thickness z is about 1.65 mm. (d) The diagram of liquid replacement setup in the pig eye experiments. It is made by an infusion device and two needles. We made 50mL glucose solution flow through the anterior chamber each time.

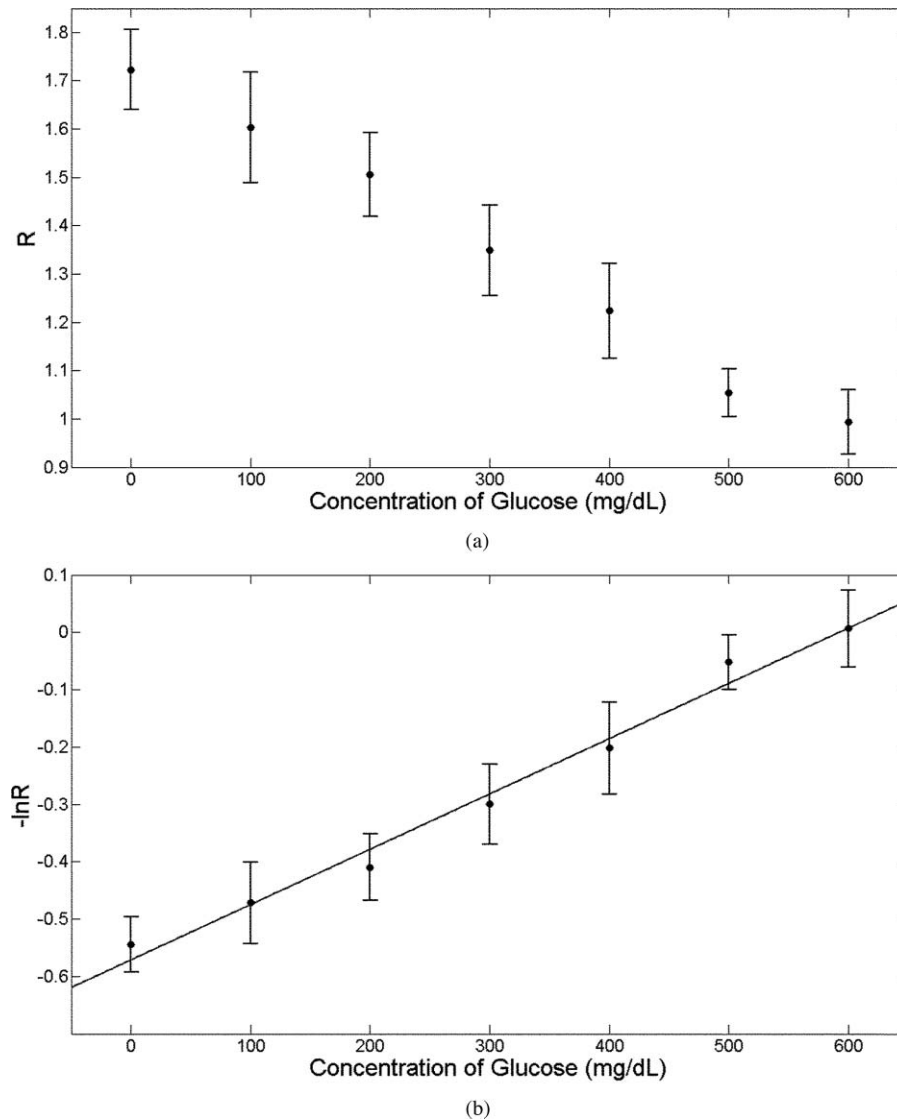


Fig. 7 The measurement results for the pig eye experiment: (a) The R is shown versus glucose concentration. We recorded 30 R within 2 min for a sample measurement. We took an average for these 30 R we got each time. Due to the limitation of the eyes *ex vivo*, each of the concentration was only measured once. The resolution was 69.6 mg/dL, and the RMSEP was 65.62 mg/dL. (b) The $-\ln R$ is shown versus glucose concentration. The black line represents the fit of the data points. The linear correlation between C and $-\ln R$ was 0.9931.

can be introduced to improve the resolution. (1) We can select other light sources to get a higher value of $\Delta\mu_a$. For example, the light source with wavelength at 1625 nm can be replaced by the light source with wavelength at 2100 nm, where glucose has a three times higher absorption.³⁰ (2) The light incidence position can be changed to obtain a larger value of z . One possible solution is using a high intensity light to shine on eyes to make the pupil smaller before experiment. Then we could make the incident light closer to the center and obtain a larger value of z . The resolution can thus be enhanced with the larger depth z . Moreover, the depth z can be enhanced if we utilize obliquely incident light instead of current normally incident mode. As a conclusion, the resolution may be potentially improved to meet the clinical application.

5 Conclusion

We developed a differential absorption low-coherent interferometry (DALCI) technique to measure the glucose concentration

in the anterior chamber of eye model. The results demonstrated that the intensity of emergent light of wavelength 1625 nm was declined whereas the intensity of emergent light of wavelength 1310 nm was unchanged with the glucose concentration increasing. In the pig eye experiment, we proved that a resolution glucose level of 69.6 mg/dL can be potentially obtained *ex vivo*. The results showed an excellent linearity of $\ln R$ and glucose concentration within a range of 0–600 mg/dL. This method for measurement of glucose concentration in aqueous humor is potential to calculate the blood sugar level according to the steady relationship between the glucose concentration in aqueous humor and in blood.

Acknowledgments

This research was supported by the 863 project, China (2006AA6Z402) and the projects 61040067 and 30770592, NSFC, China.

References

1. R. J. McNichols and G. L. Coté, "Optical glucose sensing in biological fluids: an overview," *J. Biomed. Opt.* **5**(1), 5–16 (2000).
2. M. A. Arnold, "Non-invasive glucose monitoring," *Curr. Opin. Biotechnol.* **7**(1), 46–49 (1996).
3. G. B. Christison and H. A. MacKenzie, "Laser photoacoustic determination of physiological glucose concentrations in human whole blood," *Med. Biol. Eng. Comput.* **31**, 284–290 (1993).
4. Z. Zhao, "Pulsed photoacoustic techniques and glucose determination in human blood and tissue," PhD dissertation, University of Oulu, Finland (2002).
5. K. V. Larin, M. S. Eledersi, M. Motamedi, and R. O. Esenaliev, "Noninvasive blood glucose monitoring with optical coherence tomography," *Diabetes Care* **25**, 2263–2267 (2002).
6. K. Maruo, M. Tsurugi, M. Tamura, and Y. Ozaki, "In vivo noninvasive measurement of blood glucose by Near-Infrared diffuse-reflectance spectroscopy," *Appl. Spectrosc.* **57**(10), 1236–1244 (2003).
7. R. Marbach, T. H. Koschinsky, F. A. Gries, and H. M. Heise, "Noninvasive blood glucose assay by near-infrared diffuse reflectance spectroscopy of the human inner lip," *Appl. Spectrosc.* **47**, 875–881 (1993).
8. G. L. Coté, "Noninvasive and minimally-invasive optical monitoring technologies," *J. Nutr.* **131**, 1596S–1604S (2001).
9. J. R. Collins, "Change in the Infra-Red Absorption Spectrum of Water with Temperature," *Phys. Rev.* **26**(6), 771–779 (1925).
10. V. V. Sapozhnikova, R. V. Kuranov, I. Cicenaitė, R. O. Esenaliev, and D. S. Prough, "Effect on blood glucose monitoring of skin pressure exerted by an optical coherence tomography probe," *J. Biomed. Opt.* **13**(2), 021112 (2008).
11. S. Pohjola, "The glucose content of the aqueous humor in man," *Acta Ophthalmol.* **88**, 11–80 (1966).
12. B. D. Cameron, H. W. Gorde, B. Satheesan et al., "The use of polarized laser light through the eye for noninvasive glucose monitoring," *Diabetes Technol Ther* **1**(2), 135–43 (1999).
13. B. H. Malik, G. L. Cote, "Real-time, closed-loop dual-wavelength optical polarimetry for glucose monitoring," *J. Biomed. Opt.* **15**(1), 017002 (2010).
14. B. H. Malik, G. L. Cote, "Modeling the corneal birefringence of the eye toward the development of a polarimetric glucose sensor," *J. Biomed. Opt.* **15**(3), 037012 (2010).
15. J. L. Lambert, C. C. Pelletier, M. Borchert, "Glucose determination in human aqueous humor with Raman spectroscopy," *J. Biomed. Opt.* **10**(3), 031110 (2005).
16. C. C. Pelletier, J. L. Lambert, and M. Borchert, "Determination of glucose in human aqueous humor using Raman spectroscopy and designed-solution calibration," *Appl. Spectrosc. C* **59**(8), 1024–1031 (2005).
17. A. J. Webb, B. D. Cameron, "Multivariate image processing technique for noninvasive glucose sensing," *Proc. SPIE* **757203** (2010).
18. Y. Liu, P. Hering, M. O. Scully, "An integrated optical sensor for measuring glucose concentration," *Appl. Phys. B* **54**(1), 18–23 (1992).
19. D. Huang, E. A. Swanson, C. P. Lin, J. S. Schuman, W. G. Stinson, W. Chang, M. R. Hee, T. Flotte, K. Gregory, C. A. Puliafito, and J. G. Fujimoto, "Optical coherence tomography," *Science* **254**(5035), 1178–1181 (1991).
20. M. Pircher, E. Götzinger, R. Leitgeb, A. F. Fercher, and C. K. Hitzenberger, "Measurement and imaging of water concentration in human cornea with differential absorption optical coherence tomography," *Opt. Express* **11**, 2190–2197 (2003).
21. T. Støren, A. Røyset, L. O. Svaasand, T. Lindmo, "Measurement of dye diffusion in scattering tissue phantoms using dual-wavelength low-coherence interferometry," *J. Biomed. Opt.* **11**(1), 014017 (2006).
22. E. A. Boettner and J. R. Wolter, "Transmission of the ocular media," *Invest. Ophthalmol.* **1**(6), 776–783 (1962).
23. S. F. Malin, T. L. Ruchti, T. B. Blank, S. N. Thennadil, and S. L. Monfre, "Noninvasive prediction of glucose by near-infrared diffuse reflectance spectroscopy," *Clin. Chem.* **45**(9), 1651–1658 (1999).
24. F. Y. Sun and Z. J. Sun, *The Medical Handbook of Eye Disease*, Dalian University of Technology Press, Da Lian (2007).
25. T. C. Ye and N. L. Wang, *The atlas of clinical glaucoma*, People's Medical Publishing House, Bei Jing (2007).
26. H. N. Zhu, *Introduction of New-concept experimental measurement of physics—The basis of Data Analysis and Evaluation of Uncertainty*, Higher Education Press, Bei Jing (2007).
27. R. O. Esenaliev, K. V. Larin, I. V. Larina, and M. Motamedi, "Noninvasive blood glucose monitoring with optical coherence tomography," *Opt. Lett.* **26**(13), 992–994 (2001).
28. Pipe & Rapley, *Ocular Anatomy and Histology*, The association of British Opticians, London (1999).
29. R. Poddar, J. T. Andrews, P. Shukla, and P. Sen, "Noninvasive glucose monitoring techniques: a review and current trends," arXiv: 0810.5755v1 [physics.med-ph] (2008).
30. V. V. Tuchin, "Handbook of optical sensing of glucose in biological fluids and tissues," Taylor & Francis Group, LLC, (2009).
31. B. Rabinovitch, W. F. March, and R. L. Adams, "Noninvasive glucose monitoring of the aqueous humour of the eye," *Diabetes Care* **5**, 254–265 (1982).
32. Benon H. J. Bielski, David A. Comstock, and Richard A. Bowen, "Ascorbic Acid Free Radicals. I. Pulse Radiolysis Study of Optical Absorption and Kinetic Properties," *J. Am. Chem. Soc.* **93** (22), 5624–5629 (1971).
33. N. Kollias, "The spectroscopy of human melanin pigmentation," In: *Melanin: Its Role in Human Photoprotection*, 31–38 Valdenmar Publishing Co. (1995).
34. A. Vogel, C. Dlugos, and R. Nuffer, "Optical properties of human sclera, and their consequences for transscleral laser applications," *Lasers in Surgery and Medicine* **11**(4), 331–340 (1991).
35. P. Wistrand, J. Stjernschantz, and K. Olsson, "The incidence and time-course of latanoprost-induced iridial pigmentation as a function of eye color," *Survey of Ophthalmology* **41**(S2), S129–S138 (1997).
36. D. M. Haaland and E. V. Thomas, "Partial least-squares methods for spectral analysis I: relation to other quantitative calibration methods and the extraction of qualitative information," *Anal. Chem.* **60**, 1193–1202 (1988).
37. H. M. Heise, R. Marbach, G. Janatsch, and J. D. Krse-Jarres, "Multivariate determination of glucose in whole blood by attenuated total reflection infrared spectroscopy," *Anal. Chem.* **61**, 2009–2015 (1989).
38. H. Martens and T. Naes, *Multivariate Calibration*, Wiley, Chichester (1991).
39. T. W. King, G. L. Cot, R. McNichols, and M. J. Goetz, Jr., "Multispectral polarimetric glucose detection using a single pockels cell," *Opt. Eng.* **33**(8), 2746–2753 (1994).
40. G. R. Reiss, D. A. Lee, J. E. Topper, R. F. Brubaker, "Aqueous humor flow during sleep," *Invest. Ophthalmol. Vis. Sci.* **25**, 776 (1984).